Supplementary Information

Chromonic Nematic Liquid Crystals in a Room-Temperature Ionic Liquid

J. R. Magana[a], A. Pérez-Calm[a,b], C. Rodriguez-Abreu[a,b]

[a] Institute for Advanced Chemistry of Catalonia (IQAC), Spanish National Research Council (CSIC), Jordi Girona 18-26 08034, Barcelona, Spain.

[b] Networking Research Center on Bioengineering, Biomaterials and Nanomedicine (CIBER-BBN), Jordi Girona 18-26 08034, Barcelona, Spain.

Experimental

CHEMICALS

Commercially available perylenetetracarboxylic dianhydride >98% (PTCDA, TCI Europe), hydroxyethylammonium formate (HEAF, Iolitec), ethyl ammonium nitrate (EAN, Iolitec) and 1-ethyl-3-methylimidazolium acetate (EMIAc, Iolitec), Tetraethyl-orthosilicate (TEOS, Sigma Aldrich) were used without further purification. Ultrapure water (resistivity = 18 MΩ/cm) was used in all experiments. Dyes and chromonic mesogens used in the experiments were obtained from different manufacturers (see Table SI1) at the highest purity available and used without further purification.

SYNTHESIS

Bis (N',N' - diethyl - N' - methyl – 2 - ammoniumethyl) perylene – 3 , 4 , 9 , -10 - tetracarboxylic diimide dichloride (PDI), was synthesized according to the literature.[1]

UV-VIS SPECTROSCOPY

UV-vis spectra were collected in a Shimadzu UV-2550 and a Perkin Elmer Lambda 365 using a quartz cuvette with a path length of 2 mm. The absorbance, *A*, was converted into the molar absorption coefficient, *ε*, using:

$$A = \varepsilon c l$$

Where *c* and *l* are the dye concentration and cuvette path length, respectively. The PDI spectra in HEAF and water was modeled assuming an isodesmic aggregation similar to previous publications by using the following equation:[2]

$$\epsilon(\lambda, C_o) = (\varepsilon_M(\lambda) - \varepsilon_D(\lambda))\frac{\sqrt{(8K_D C_o + 1)} - 1}{4K_D}$$

Where ε_M and ε_D are the molar absorption coefficient of the monomer and dimer, respectively, K_D is the dimerization constant, and C_o is the total molar concentration of PDI in solution. The values for K_D were averaged from different wavelengths and different concentrations. The Gibbs free energy, *ΔG*, was calculated as:

$$\Delta G = \frac{k_B T * ln(K_D)}{N_a}$$

Where *T*, k_B and N_a are the absolute temperature, the Boltzmann constant, and the Avogadro number, respectively.

K_D, calculated as a function of temperature, was used to estimate the activation energy, E_a, according to Arrhenius theory:

$$\ln(K_D) = -\frac{E_a}{k_B T} + intercept$$

FLUORESCENCE SPECTROSCOPY

Samples were measured in 2mm quartz cuvettes in a Horiba Scientific Fluoromax-4 and an Agilent Cary Eclipse. The conditions where identical for all the measurements and the data is as obtained without any normalization.

SAMPLE PREPARATION AT HIGH PDI CONCENTRATIONS.

PDI/HEAF viscous samples (above 25 wt% PDI) were prepared by repeatedly passing the mixture through a narrow constriction in flame sealed glass tubes using a centrifuge.

SMALL ANGLE X-RAY SCATTERING

All experiments were performed on an Anton Paar SAXSess MC^2 system. The scattering intensity was measured as a function of the scattering vector, q:

$$q = \frac{4\pi * sin(\theta)}{\lambda}$$

where θ is the scattering angle and l is the radiation wavelength (1.54 Å).

Liquid crystalline PDI samples were placed in flame-sealed glass capillaries. The intercolumnar distance, d, in the nematic phase was estimated using Bragg law as:

$$d = \frac{2\pi}{q_{max}}$$

Where q_{max} is the q value at the peak maxima. The cross-sectional area of the aggregates, A_c, can be estimated by approximating the nematic phase to a loose hexagonal packing as:[3]

$$A_c = \frac{2d^2\phi_f}{\sqrt{3}}$$

Where ϕ_f is the volume fraction (estimated using the density of mesogen in the solid state).

POLARIZED OPTICAL MICROSCOPY

Polarized optical microscopy (POM) observations were made on a Nikon SMZ-1500 microscope. Temperature-dependent POM was performed on an Olympus BX51TRF6 microscope coupled to a Peltier hot stage with a precision of ±1 °C.

SCANNING ELECTRON MICROSCOPY

SEM micrographs of the silica samples were collected using a Hitachi TM4000Plus II operating 5 kV with secondary electrons. Samples were prepared by drop-casting ethanol dispersions on a silicon wafer.

NITROGEN ADSORPTION-DESORPTION

Nitrogen adsorption and desorption studies were performed on an Autosorb-1 Quantachrome Instrument.

Table SI1. Dyes, chromonic mesogens and ILs used in POM contact experiments. Manufacturers are indicated between brackets next to the mesogen´s name. Last column displays the occurrence of such mesogens in water and their concentration range (if known) at 20 °C

Chromonic mesogen	**Molecular structure**	**HEAF** 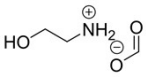	**EMIAc** 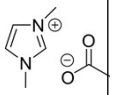	**EAN** 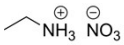	**LCLC formation in water [wt% range]**
Acid Red 27 (TCI)	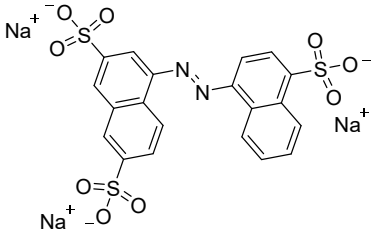	No LC	Not tested	Not tested	[0.5 wt% – 10 wt%] [4]
Congo Red (TCI)	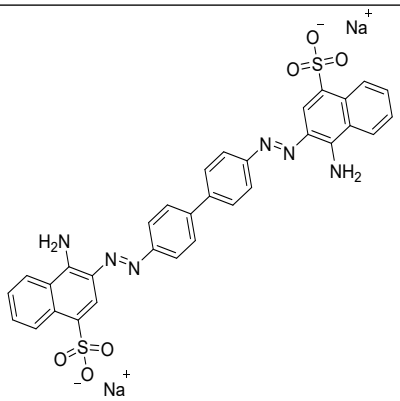	No LC	Not tested	Not tested	LC[5,6]
Neutral Red (Sigma-Aldrich)	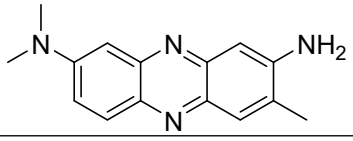	No LC	No LC	Not tested	LC(unpublished results)
Acid Black 1 (TCI)	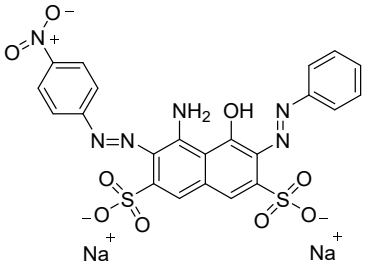	No LC	Not tested	Not tested	No LC

Alcian Blue tetrakis (methylpyridinium) chloride aka Alcian Blue (Sigma-Aldrich)	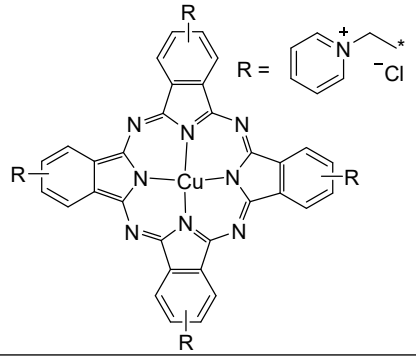	No LC	No LC	Not tested	LC (unpublished results)
1,1'-Diethyl-3,3,3',3'-tetramethylindocarbocyanine Iodide (TCI)	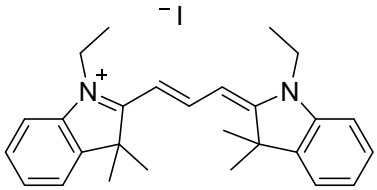	No LC	Not tested	Not tested	Not tested
3,3,3',3'-Tetramethyl-1,1'-bis(4-sulfobutyl) indocarbocyanine(TCI)	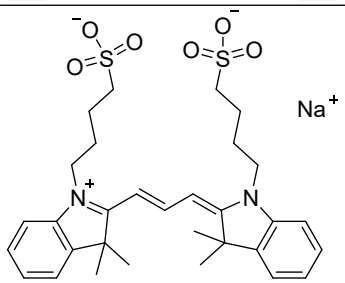	No LC	Not tested	Not tested	No LC
AzBTS (TCI)	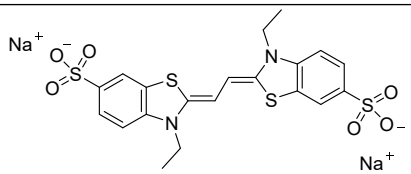	No LC	Not tested	Not tested	No LC
Nickel(II) phthalocyanine-tetrasulfonic acid tetrasodium salt (Sigma-Aldrich)	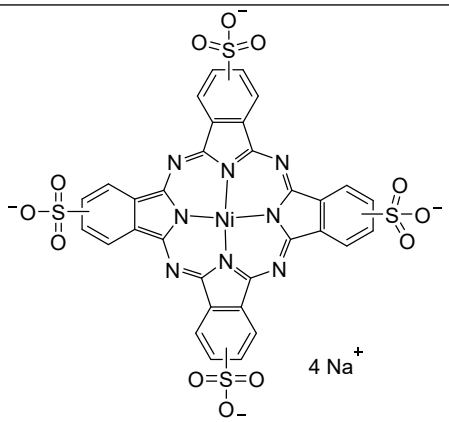	No LC	Not tested	Not tested	LC[7]

Copper phthalocyanine-3,4',4",4"-tetrasulfonic acid tetrasodium salt (Sigma-Aldrich)	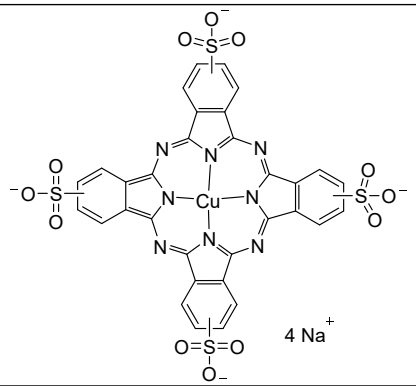	No LC	Not tested	Not tested	LC[7]
Cromolyn (Alfa Aesar)	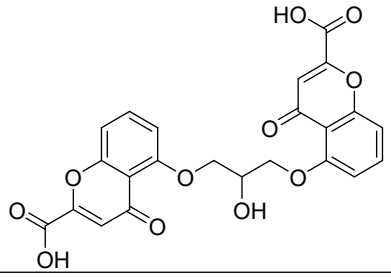	No LC	No LC	Not tested	[5 wt% - 40 wt%][8]
Sunset Yellow (Sigma-Aldrich)	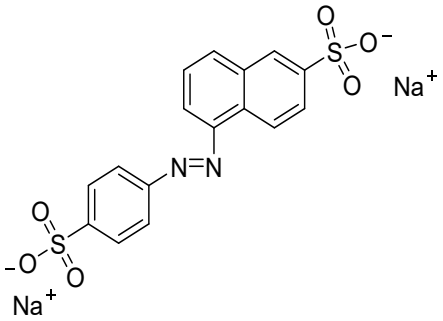	No LC	Not tested	Not tested	[25 wt% – 45 wt%][9]
Pyronin Y (Sigma-Aldrich)	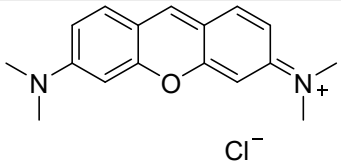	No LC	No LC	No LC	[40 wt% - 75wt %][3]
Quinaldine Red Iodide (Sigma-Aldrich)	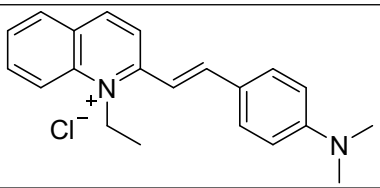	No LC	No LC	Not tested	No LC
Quinaldine Red Acetate (Synthesized)	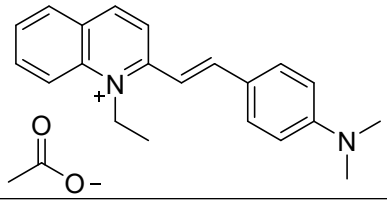	No LC	No LC	Not tested	[35 wt% - 70 wt%][3]

Pinacyanol Acetate (Synthesized)	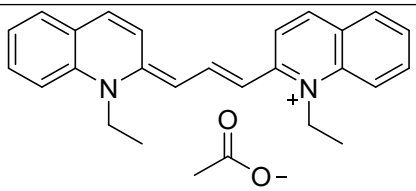	LC (metastable)	No LC	No LC	[<1 wt% -10 wt%][10]
Pinacyanol Chloride (Sigma-Aldrich)	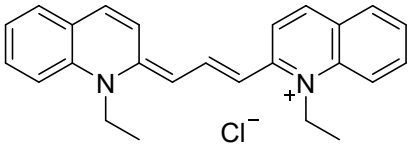	LC (metastable)	Not tested	Not tested	No LC
Gallocyanine (Sigma-Aldrich)	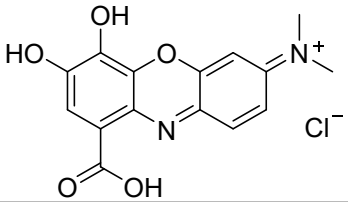	No LC	No LC	Not tested	No LC
Perylene diimide chloride (PDI) (Synthesized)	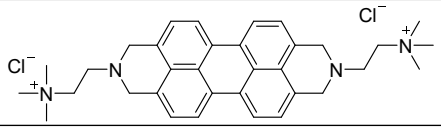	LC (stable)	No LC	No LC	[5 wt% - 20 wt%][11]
Diethyl (thiacarbocyanine) acetate (Synthesized)	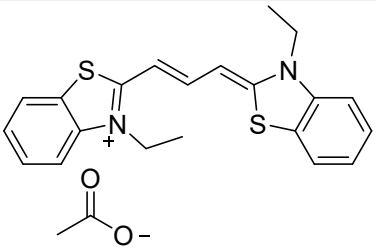	LC	Not tested	Not tested	LC [2]
Diethyl (thiacarbocyanine) Iodide (TCI)	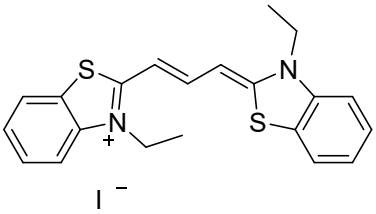	No LC	Not tested	Not tested	No LC
Dipropyl (thiacarbocyanine) acetate (Synthesized)	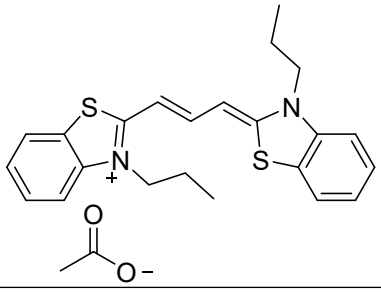	LC	Not tested	Not tested	LC[2]
Dipropyl (thiacarbocyanine) Iodide (TCI)	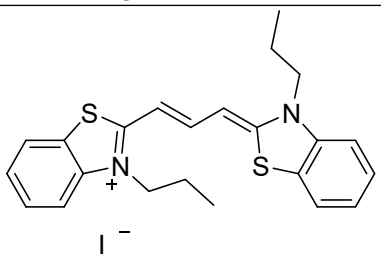	No LC	Not tested	Not tested	No LC

Dibutyl (thiacarbocyanine) acetate (Synthesized)	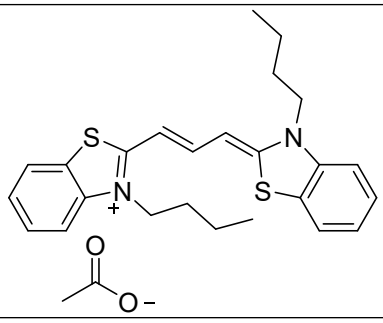	LC	Not tested	Not tested	LC[2]
Dibutyl (thiacarbocyanine) Iodide (TCI)	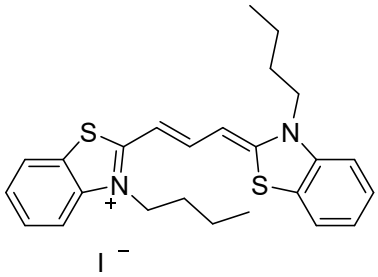	No LC	Not tested	Not tested	No LC

Table SI2. Thermodynamic parameters calculated from the UV-vis spectra.

Sample	K_D (M^{-1})	$-\Delta G$ (kJ/mol)	E_a (kJ/mol)
PDI in HEAF	$5.2 \cdot 10^3 \pm 1.3 \cdot 10^3$	21.2	12.2
PDI in water	$1.4 \cdot 10^5 \pm 8.0 \cdot 10^4$	29.4	7.7

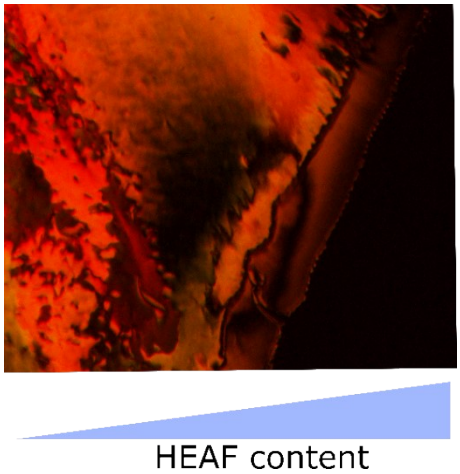

Figure SI1. Representative POM micrograph at room temperature (25°C) of the contact interface between PDI and HEAF.

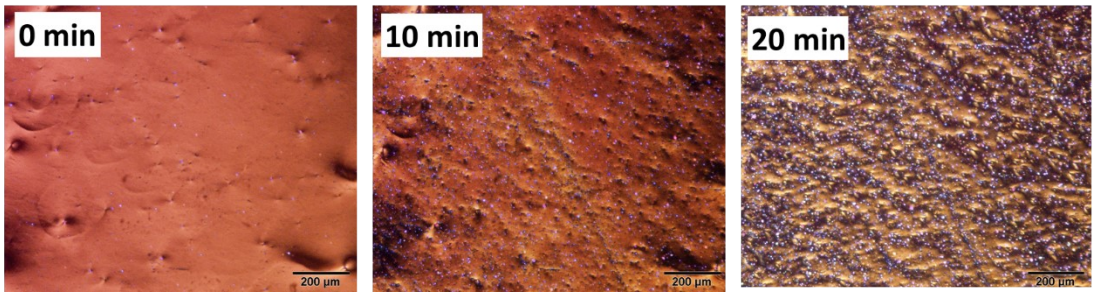

Figure SI2. POM micrographs at room temperature (25°C) of a 3 wt% Pinacyanol acetate in HEAF displaying the crystallization over time of a nematic mesophase. The scale bar is 200 µm

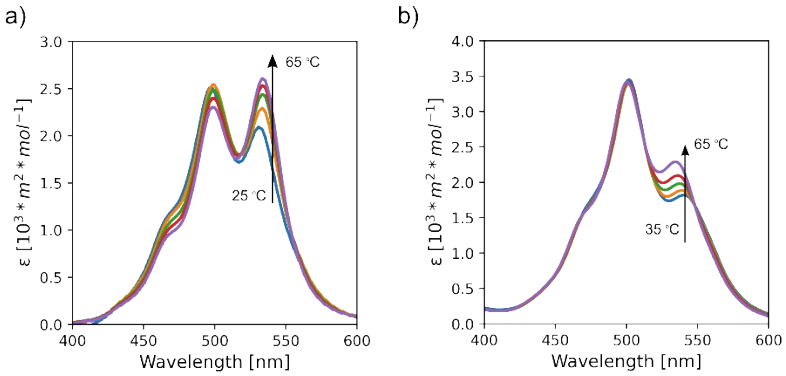

Figure SI3. Temperature-dependent UV-Vis spectra of a 100 µM PDI solution in a) HEAF and b) water.

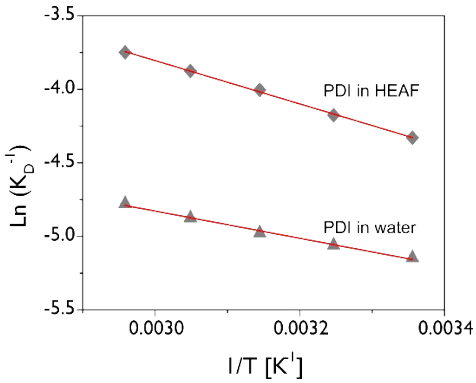

Figure SI4. Arrhenius plot showing the natural logarithm of the dimerization constant vs the inverse temperature of a 100 µM PDI sample in HEAF and water.

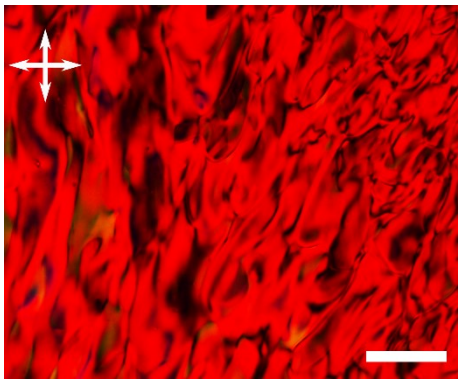

Figure SI5. POM micrograph of a 30 wt% PDI sample in HEAF at room temperature showing a characteristic Schlieren texture (scale bar = 100 µm).

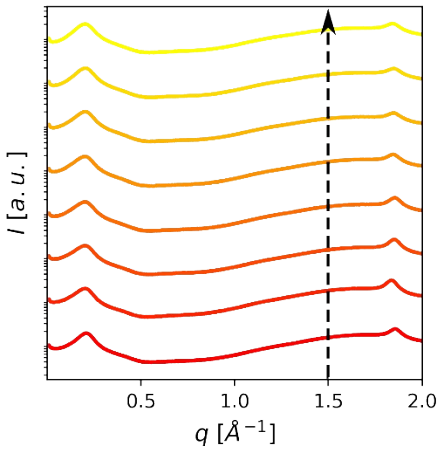

Figure SI6. Temperature-dependent SWAXS patterns of a 30 wt% PDI sample in HEAF heated from 25 °C to 95 °C in 10 °C steps; the arrow indicates increasing temperature.

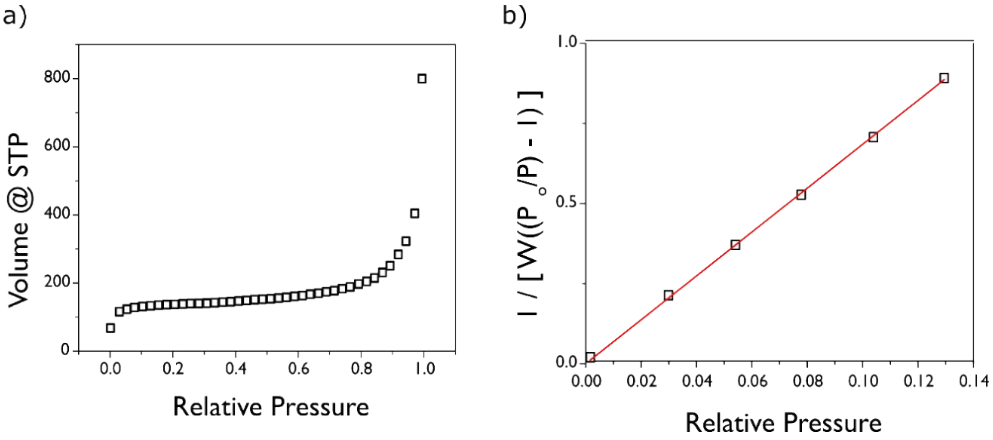

Figure SI7. a) Nitrogen adsorption isotherm of the calcined silica material and b) the corresponding fit for the Brunauer-Emmer-Teller (BET) theory.

References

[1] S. W. Tam-Chang, J. Helbley, I. K. Iverson, *Langmuir* **2008**, *24*, 2133–2139.

[2] J. R. Magana, C. Solans, L. M. Salonen, E. Carbó-Argibay, J. Gallo, G. J. T. Tiddy, C. Rodríguez-Abreu, *J. Taiwan Inst. Chem. Eng.* **2018**, *92*, 134–142.

[3] J. R. Magana, M. Homs, C. Solans, M. Obiols-Rabasa, L. M. Salonen, C. Rodríguez-Abreu, *J. Phys. Chem. B* **2016**, *120*, 250–258.

[4] A. Alfutimie, A. P. Ormerod, J. W. Jones, H. Wheatcroft, D. J. Edwards, G. J. T. Tiddy, *http://dx.doi.org/10.1080/02678292.2015.1024770* **2015**, *42*, 1169–1178.

[5] M. R. Kuzma, V. Skarda, M. M. Labes, *J. Chem. Phys.* **1998**, *81*, 2925.

[6] M. Skowronek, B. Stopa, L. Konieczny, J. Rybarska, B. Piekarska, E. Szneler, G. Bakalarski, I. Roterman, *Biopolymers* **1998**, *46*, 267–281.

[7] Carlos Rodríguez-Abreu, Y. V. Kolen'ko, Kirill Kovnir, Margarita Sanchez-Dominguez, R. Goswami Shrestha, Partha Bairi, Katsuhiko Ariga, L. Kumar Shrestha, *Phys. Chem. Chem. Phys.* **2020**, *22*, 23276–23285.

[8] N. H. Hartshorne, G. D. Woodard, *https://doi.org/10.1080/15421407308083381* **2007**, *23*, 343–368.

[9] D. J. Edwards, J. W. Jones, O. Lozman, A. P. Ormerod, M. Sintyureva, G. J. T. Tiddy, *J. Phys. Chem. B* **2008**, *112*, 14628–14636.

[10] C. Rodríguez-Abreu, C. A. Torres, G. J. T. Tiddy, *Langmuir* **2011**, *27*, 3067–3073.

[11] S. W. Tam-Chang, I. K. Iverson, J. Helbley, *Langmuir* **2003**, *20*, 342–347.